Screening of the topological charge in a correlated instanton vacuum

E.V. Shuryak and J.J.M. Verbaarschot
Department of Physics, State University of New York, Stony Brook, New York 11794
(Received 31 October 1994)

Screening of the topological charge due to fermion-induced interactions is an important phenomenon, closely related with the resolution of the strong CP and U(1) problems. We study the mechanism of such screening in a "correlated instanton vacuum," as opposed to the "random" one. Both scalar and pseudoscalar gluonic correlators are analyzed by means of an observable that minimizes finite size effects. Screening of the topological charge is established. This allows us to calculate the η' mass without having to invert the Dirac operator. We suggest that this method might be used in lattice QCD calculations as well. Our results for the screening of the topological charge are in agreement with the chiral Ward identities, and the scalar gluonic correlator satisfies a low energy theorem first derived by Novikov *et al.* We also propose a modified Witten-Veneziano formula, in which the topological susceptibility is not defined for an *infinite* box in a world *without* fermions, but for *small* box in the real world.

PACS number(s): 12.38.Lg, 12.38.Gc

I. INTRODUCTION

Tunneling between topologically distinct sectors of the gauge field, described semiclassically by instantons [1,2], is known to be one of the major nonperturbative phenomena in QCD. Their importance was significantly clarified in the last few years. In particular, a large set of QCD correlation functions was studied [3–5] in the so-called "random instanton liquid model" (RILM). The results are in surprisingly good agreement both with experiment (see [6]) and lattice data [7]. They clearly show that many hadrons (including, e.g., pions and nucleons) are actually bound by the instanton-induced interactions, and their properties such as masses and wave functions [8] can be well reproduced by the simplest instanton-based model.

Second, important new results were obtained from the study of "cooled" lattice configurations. ("Cooling" is a procedure that relaxes a given gauge field configuration to its closest "classical version.") The nonperturbative classical fields were found to be the superposition of instantons [9]. Furthermore, the recent work of Chu *et al.* [10] has essentially reproduced the key parameters of the "instanton liquid" picture of the QCD vacuum: the mean instanton separation $R \approx 1.1$ fm and the typical instanton radius $\rho \approx 0.35$ fm, about 10% off the values suggested by one of us a decade ago [11]. They also demonstrated explicitly how hadronic correlators survive cooling, and gave quite convincing arguments showing that confinement effects play only a relatively minor role.

In spite of such progress in phenomenology and lattice studies, a consistent quantitative theory of instanton-induced phenomena is still missing. The model mentioned above, the RILM, assumes random instanton positions and orientations. It is the simplest possible model, which ignores all effects related to instanton interactions. It seems to be a good approximation for many phenomena, but a few exceptions should be mentioned.

In particular, *finite temperature* phenomena related to the chiral symmetry restoration transition cannot be understood without the introduction of strong correlations between instantons and anti-instantons [12]. Furthermore, in the phase above T_c these correlations are so strong that they lead to breaking of the liquid into a set of weakly interacting $\bar{I}I$ "molecules."

In this paper we discuss a global manifestation of the quark-induced interaction between instantons in the vacuum ($T = 0$) case. It is known that (in the chiral limit) it should screen *large-scale* fluctuations of the topological charge. As it is a very spectacular manifestation of *quark-induced dynamical correlations*, it is natural to start our new series of studies of instanton-induced phenomena by reporting these results first. A detailed report on properties of the correlated instanton vacuum, including correlation functions and wave functions in particular channels, will be published elsewhere [13].

Before we proceed, let us recall why fluctuations of the topological charge are of interest. It is well known that strong interactions conserve CP to a high accuracy. Two ways to understand this "fine-tuning" were suggested. First, the θ parameter may set itself to *zero* due to the axion mechanism [14]. A new suggestion by Schierholz [15] is that $\theta = 0$ may happen to be a phase transition point. In any case, there are all kinds of open questions related to QCD at nonzero values of θ, say whether or not it is even a confining theory, see [15].

The second possibility is that the value of θ may be *irrelevant* because the total topological charge of the vacuum is screened completely. This happens if at least one quark flavor is massless, but this does not seem to be the case in the real world. A new proposal was put forward by Samuel [16] who argued that the interaction between instantons may screen the topological charge for *nonzero* quark masses, below some critical mass value.

Another important aspect is the famous U(1) problem [17,18], related to properties of the η' meson. Phenomenologically, its detailed properties are very impor-

tant, for example, for understanding of the so-called "proton spin crisis." Theoretically, a recent discussion in connection with the Samuel mechanism can be found, e.g., in [19,20] in which the exchange of an η' was interpreted as a mediator of the Debye-type screening. Generally speaking, the "screening" phenomenon puts significant constraints on the parameters of this meson. Finite temperature effects in relation to the interpretation of the η' particle as an inverse screening length were discussed in [21].

A famous approach to the U(1) problem is based on the Witten-Veneziano formula [22,23] relating the parameters of the η' to the topological susceptibility χ. Although it clearly explains qualitative features of the phenomenon, we cannot be satisfied by its present formulation. It is very difficult to make such a type of relation quantitative because the two sides of the equation "live in two different worlds" [19]. The parameters of the η' meson are obtained from experiment and refer to the real world, while χ is calculated either in the large N_c limit, or in quenched QCD [24], or in other nonscreened theories. (Endless discussions of how one should match the units on both sides were made, and in practice people simply use some unjustified conventions.)

No convincing lattice measurements of the η' properties in QCD with dynamical fermions exist so far.[1] In this paper we propose a method that does not require the inversion of the Dirac operator and might therefore be useful for lattice simulations.

The results of the η' correlator in the RILM [3–5] are also unsatisfactory: the corresponding channel has shown to produce a too strong $\bar{q}q$ repulsion. In addition to that, the random ensemble has obviously no screening, so one cannot get any constraints related to it. Therefore, in this paper we study an ensemble of "interacting instantons," and test whether and how the corresponding relations hold. An alternative approach to gluonic correlation functions, both in random and correlated instanton vacua, is developed in [26].

We suggest that the best way to clarify the issue is to study the dependence of *topological susceptibility* $\chi(V)$ defined in the *subvolume* V. Its dependence on V, as well as on the quark masses m_f, are the main objective of our work. The screening of the topological charge[2] implies that, *for large* $V, \chi(V)$ is proportional to the *area* of V instead of $\chi(V) \sim V$. However, for small volumes one always has that $\chi(V) \sim V$. The crossover point between these two regimes defines a screening length, identified as the inverse η' mass.

In Sec. II we define the instanton liquid model and discuss the parameters used in our calculations. In Sec. III the Debye cloud of a topological charge is studied and in Sec. IV the volume dependence of the topological susceptibility is evaluated. These results are analyzed in the context of correlators that follow from effective field theory (see Appendix B). In Sec. V we discuss the scalar gluonic correlation function which is related to the fluctuations of the total number of instantons in a given volume. Concluding remarks are made in Sec. VI.

II. THE MODEL

The basis of this work is the "interacting instanton liquid model" (IILM), formulated as a particular statistical model amenable for numerical simulations [28–30] or analytical studies [31,32]. The partition function for $N/2$ instantons and $N/2$ anti-instantons is generally given by

$$Z = \int \prod_{I=1}^{N} d\Omega_I dz_I d\rho_I \mu(\rho_I) \prod_f^{N_f} \det(T + im_f) \times \exp\left[-\beta(\rho\Lambda) \sum_{I<J} S_{IJ}^{\rm int}\right], \tag{2.1}$$

where Ω_I, z_I, and ρ_I, denote the orientation, position, and size of pseudoparticle I, respectively. The size distribution $\mu(\rho)$ contains a factor $\sim \rho^{b-5}$ (with the standard β-function parameter $b = \frac{11}{3}N_c - \frac{2}{3}N_f$) due to the Jacobian of the transformation to collective coordinates and the leading quantum corrections. The QCD parameter Λ in $\beta(\rho\Lambda) = -b\ln(\rho\Lambda)$ will be determined phenomenologically.

The main dynamical effects we are going to study are due to the determinant of the Dirac operator. In the subspace of the zero modes it can be expressed in terms of the overlap matrix elements T, which for the "streamline" gauge fields [33] are given by [34] (see Appendix A for a derivation)

$$T_{IA}(\rho_I\rho_A)^{1/2} = (\rho_I\rho_A)^{1/2} \int d^4x \psi_0^{\dagger I}(x) i\hat{D} \psi_0^A(x) = -\tfrac{1}{2}{\rm Tr}(\tau_\mu^+ \hat{R}_\mu^{IA} U_I^{-1} U_A) F(\lambda), \tag{2.2}$$

where the scalar function $F(\lambda)$ is defined by

$$F(\lambda) = 6\int_0^\infty \frac{dr r^{3/2}}{(r+1/\lambda)^{3/2}(r+\lambda)^{5/2}}, \tag{2.3}$$

and $\hat{R}_\mu^{IA} = R_\mu^{IA}/R^{IA}$. $F(\lambda)$ depends only on the conformally invariant combination

$$\lambda = \frac{1}{2}\left(\tilde{R}^2 + \frac{\rho_I}{\rho_A} + \frac{\rho_A}{\rho_I}\right) + \frac{1}{2}\left[\left(\tilde{R}^2 + \frac{\rho_I}{\rho_A} + \frac{\rho_A}{\rho_I}\right)^2 - 4\right]^{1/2}, \tag{2.4}$$

where $\tilde{R} = R/\sqrt{\rho_I\rho_A}$. Asymptotically, for large R/ρ, the $T_{IA} \sim 4\rho^3/R^3$ (the geometric average of ρ_I and ρ_A is denoted by ρ).

[1] The best one so far is reported in [25], where the η' mass was calculated in *quenched* lattice gauge theory using a rather indirect method.

[2] See also [27], where this phenomenon was discussed for the Schwinger model.

Considering the interaction due to gauge fields, let us first mention that we deviate from previous works[3] by using the interaction derived in [33] from the so-called "streamline equation" [35]. They correspond to the true bottom of the valley for the $\bar{I}I$ configurations. This interaction differs from the previously used ones in one important aspect: for one relative orientation the repulsive "core" at small distances is gone. Our numerical simulations have confirmed earlier suspicions that it leads to an "overcorrelated liquid" of close $\bar{I}I$ pairs.[4] Thus, it seems that the original hopes to stabilize the ensemble at the purely classical level [31] are not satisfied. Presumably quantum effects (especially subtraction of perturbative contributions, relevant for close instanton-anti-instanton pairs with a strongly attractive interaction) will generate the effective repulsion. Two recent developments should be mentioned in this context. First, Diakonov and Petrov calculated the instanton interaction from the semiclassical quark scattering amplitude [36] and found a short range repulsion. However, at the moment it is not yet clear to what extent this interaction is of relevance to the present problem. Second, some quantum corrections, discussed in [37] using the scale anomaly relation, also lead to some effective repulsion.

Lacking a detailed understanding of these effects, we have introduced a *phenomenological repulsive core*[5] to the streamline action $S^{\rm sl}(\lambda)$

$$S^{\rm int}_{IA} = \frac{A}{2\lambda^4}{\rm Tr}\mathbf{1}_2 U_I^{-1} U_A \mathbf{1}_2 U_A^{-1} U_I + S^{\rm sl}(\lambda), \qquad (2.5)$$

$$S^{\rm int}_{II'} = \frac{A}{2\lambda^4}{\rm Tr}\mathbf{1}_2 U_I^{-1} U_I' \mathbf{1}_2 U_{I'}^{-1} U_{I'}, \qquad (2.6)$$

the same for pseudoparticles of the opposite and same kind. (In the latter case the classical interaction is absent and only the hard core is included.) The strength of the core is denoted by a free parameter A, and the color traces are needed to reduce the magnitude of the interaction if two pseudoparticles belong to different SU(2) subgroups of SU(N_c).

In principle, A determines the total instanton density in terms of $\Lambda^4_{\rm QCD}$. Unfortunately, it is not known with sufficient accuracy, and therefore it is logical to do the same thing as on the lattice, namely tune those two parameters to some measured masses, and then consider others as predictions. This strategy will be used in a subsequent work on hadron spectroscopy in the IILM.

[3]They used variational trial functions for the gauge fields known as the "sum" or "ratio" ansatz.

[4]It is still possible that one may get a phenomenologically acceptable ensemble by a significant increase in the density of instantons. However, to spend a major portion of computer time simulating pairs that are not even semiclassical fluctuations is not practically reasonable or possible.

[5]Let us point out an analogy to the famous problem of nuclear matter saturation: although there is no doubt for the existence of a repulsive core for NN forces and its decisive role in the problem, its properties and physical nature is debated even today, after decades of investigations.

However, in this paper, related to only a limited number of issues, we adopt a simpler normalization prescription. For all masses, number of colors or flavors we (i) fix the total density of the instantons at $n = 1$ fm^4, roughly corresponding to the standard gluon condensate value and to lattice measurements, and (ii) the repulsive core strength is fixed to be $A = 128$, for which we obtain a *quark condensate* that is close to the empirical value. (Note that in this region the dependence on A is relatively weak.)

We simulate the partition function with a Metropolis algorithm for an ensemble of $N/2 = 32$ instantons and an equal number of anti-instantons in a box of size (2.38 fm)$^3\times$4.76 fm. We average over typically 1000 statistically independent configurations.

III. SCREENING OF THE TOPOLOGICAL CHARGE

Let us start with the evaluation of the topological charge

$$Q(l_4) = \int_{H(l_4)} d^4x \frac{g^2}{32\pi^2} F\tilde{F}(x), \qquad (3.1)$$

in a subvolume ("slice" of the box) $H(l_4) \equiv L^3 \times l_4$. It is not an easy task on a lattice, but for our instanton ensemble this simplifies to just *counting* instantons and anti-instantons with centers in the subvolume.

Our aim is to study the details of the screening phenomenon such as the *size* and *shape* of the corresponding "Debye cloud." Let us take the center of one of the anti-instantons as the origin of the coordinate system and measure the charge distribution in the rest of the system. In Fig. 1 we show results of such studies for $N_c = 3$ and $N_f = 2$ (both quarks with equal masses, given in the label of the figures). Since the total charge in the box is set to zero, the "compensating charge" contained in the slice $H(l_4)$ for large enough L_4 should approach 1 (the anti-instanton in the center is not counted).

Our data (points) do show a strong screening phenomenon, namely that most of the compensating charge is contained in a rather small slice of the box, with a width of only about 1/3 fm. That means that the correlations between instantons and anti-instantons, responsible for screening, are actually very short range ones. The relevant hadronic excitation, the pseudoscalar flavor singlet channel, should therefore be relatively heavy. Thus, our ensemble solves the U(1) problem at least qualitatively.

One more qualitative phenomenon to mention here is the observed charge oscillations around the central charge. Those are well seen for $m = 0$, and fade away for larger masses. The oscillations are clearly nonstatistical, and their appearance suggests that in the "instanton liquid" there exist correlated clusters of various sizes. Let us recall in this connection, that in many ordinary liquids one finds a local order characteristic to a crystalline phase, and that clusters can be as big as containing hundreds of atoms. This interesting topic clearly deserves further studies.

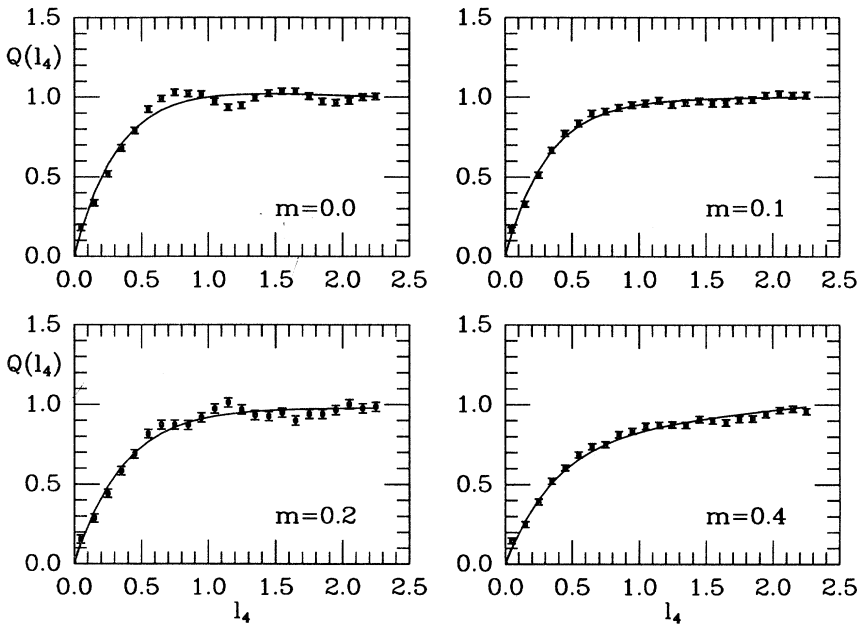

FIG. 1. The integrated topological charge in the Debye cloud of an anti-instanton in a slice of length l_4 in the four-direction of total length $2L$. The results are for $N_c = 3$ and two flavors with masses (in units of fm^{-1}) as given in the label of the figure.

Doing a more quantitative analysis, we have fitted these data by the function

$$Q(l_4) = \alpha^2[1 - \exp(-m_{\eta'} l_4)] + (1 - \alpha^2)\frac{l_4}{L}. \qquad (3.2)$$

The fraction α is the magnitude of the "compensating charge," if $\alpha = 1$ the charge is screened completely. The second term corresponds to the remaining charge which is assumed to be distributed homogeneously over the box. The first term is obtained by integrating the correlation function (B13) for fixed $x_4 - y_4 = l_4$ and $\phi = 0$. In the effective low energy field theory (discussed in Appendix B) the mass $m_{\eta'}$ is identified as the η' mass.

The obtained values for α^2 are 1.0, 0.99, 0.96, and 0.80 for the 4 masses used (m =0.0, 0.1, 0.2, and 0.4 in units of fm^{-1}), with statistical errors about 0.05. Thus, the nonscreened charge $(1 - \alpha^2) \sim m^\delta$ with the power $\delta = 1$ to 2. This conclusion should be compared to the conventional wisdom, according to which it should be proportional to the lightest quark mass. We do not know whether there is a discrepancy, or that it is due to finite size effects [the $1/L$ term in (3.2)]. In the scenario proposed by Samuel, the effect should vanish at a nonzero critical mass $(1 - \alpha^2) \sim (m - m_c)^\delta$. Our results lead to an upper limit of about $m_c < 20$ MeV.

The value of the second parameter, $m_{\eta'}$ equals 673, 623, 555, and 518 MeV, in these four cases, respectively.[6] The result is that singlet mass *decreases* with the current quark mass and suggests that the screening length becomes larger if one is increasing *all* quark masses.

IV. FLUCTUATIONS OF THE TOPOLOGICAL CHARGE IN A SUBVOLUME

In this section we switch to more conventional observables, which have been discussed in both theoretical and lattice literature. They are closely related to what was done above, but at the same time they do not demand the charge to be localized.

Although the average value of the topological charge in some volume is, of course, zero, one may study its *fluctuations* $\langle Q^2 \rangle$. The attention in literature has been focused on the *large* volume limit of that quantity, the topological susceptibility

$$\chi = \lim_{V_4 \to \infty} \frac{\langle Q^2(V) \rangle}{V_4}, \qquad (4.1)$$

but in this paper we study the *dependence* on the volume V_4. In general, one may write

$$\langle Q^2(V) \rangle = \chi(m) V_4 + \chi_3(m) A_3 + \cdots , \qquad (4.2)$$

where the subscripts refer to the dimensions of the manifolds, so the second term is proportional to the *surface* A_3, etc. The particular behavior to be observed is very informative, and can be used to extract additional information on vacuum properties (and hadronic spectroscopy). Specifically, as we try to separate *volume* from *surface* effects, we take a segment of the hypertorus of variable length l_4 along the four-axis, i.e., the slice $H(l_4)$ discussed in the previous section. Its total volume $L^3 l_4$ is proportional to l_4, while its surface area L^3 is independent of it. Because our box size in the four-direction is $L_4 = 2L$, the effective range of l_4 is $0 < l_4 < L$.

Furthermore, as we have seen in Appendix B, the topo-

[6] We remind the reader that the "MeV" makes sense in those unphysical theories only after we have defined them by some convention. Rather arbitrarily, we do this by keeping the density of instantons fixed at some value. Comparison to lattice simulations is possible, but only *after* all numbers are translated into the same convention.

logical correlation function $\Pi_P(x-y)$ [see (B13)] can be connected with parameters of the SU(3)-scalar pseudoscalar mesons, the famous η'−particle and the corresponding excited states.

Another important aspect is the dependence of χ on the quark masses m. It should be of course the same as for unscreened charge $1-\alpha^2$ discussed above: the standard scenario with the "screening of the topological charge" implies that $\chi \sim m$ at small m, while in Samuel's scenario $\chi = 0$ for all quark masses below some critical value $m < m_c$.

The fluctuations of the charge $Q(l_4)$ in the box $H(l_4)$ are obtained by integrating the correlation function (B13):

$$K_P(l_4) \equiv \langle Q(l_4)^2 \rangle = L^3 \int_{L^3} d^3x \int_{-l_4}^{l_4} dt (l_4 - |t|) \Pi_P((\vec{x}^2 + t^2)^{1/2}). \tag{4.3}$$

For finite l_4 this integration can be done as well; for sufficiently large $L \gg 1/m$ the range of the spatial integration can be extended to infinity with high accuracy $O(\exp(-Lm_{\eta'}))$ and the result is

$$\langle Q(l_4)^2 \rangle = L^3 n \left[l_4 + \cos^2\phi \frac{m_t^2}{m_{\eta'}^2} \left(\frac{1-\exp(-m_{\eta'} l_4)}{m_{\eta'}} - l_4 \right) + \sin^2\phi \frac{m_t^2}{m_\eta^2} \left(\frac{1-\exp(-m_\eta l_4)}{m_\eta} - l_4 \right) \right]. \tag{4.4}$$

This integral vanishes for $l_4 \to \infty$ if *any* quark becomes massless[7] [see Eq. (B15) in Appendix B]. For $l_4 \to 0$ we find

$$\langle Q(l_4)^2 \rangle = n L^3 l_4. \tag{4.5}$$

This result is independent of the specific shape of the subvolume, and in general we have

$$\lim_{V \to 0} \frac{\langle Q^2(V) \rangle}{V} = n. \tag{4.6}$$

Together with Eq. (B14), this results in the following formula for the η' mass:

$$m_{\eta'}^2 + m_\eta^2 - 2m_K^2 = \frac{2N_f}{f^2} \lim_{\text{small } V} \frac{\langle Q(V)^2 \rangle}{V}, \tag{4.7}$$

which is our analogue of Witten-Veneziano formula, with the topological susceptibility replaced by *local* fluctuations of the topological charge. By "small V" we mean not infinitely small volumes, of course, but those in the window between the size of a single instanton $O(\rho^4)$ and the inverse of their density $O(1/n) = R^4$.

In terms of the flavor singlet spectral function, the correlation function (4.4) implies that neither the contribution of the η (1440) nor the contribution of the continuum have been taken into account. We only calculate the nonperturbative contribution to the correlation function $\Pi_P^{\text{np}} = \Pi_P - \Pi_P^{\text{pert}}$ which implies that the contribution of the continuum and the resonances appear with opposite signs in Π_P^{np}. In particular we will find a cancellation between the ι and the continuum. In the fits to be discussed below we included the contribution of the continuum, and in all cases we found that the best fit was obtained for zero coupling of the continuum. From now on we do not include it in our discussion.

Our results for the fluctuations of the topological charge, $K_P(l_4)$, in a slice with length l_4 are shown in Figs. 2–4. The first qualitative point we would like to make is that the data points clearly show the expected transition from a *linear dependence* on l_4 (for small box size) to a *constant* for larger boxes (in case the quark mass is zero). These data points deviate drastically from the full line corresponding to randomly positioned instantons.[8] Thus, the topological charge is in fact *screened* and its fluctuations *become* a surface rather than a volume phenomenon, as soon as the quark-induced interactions are "unquenched."

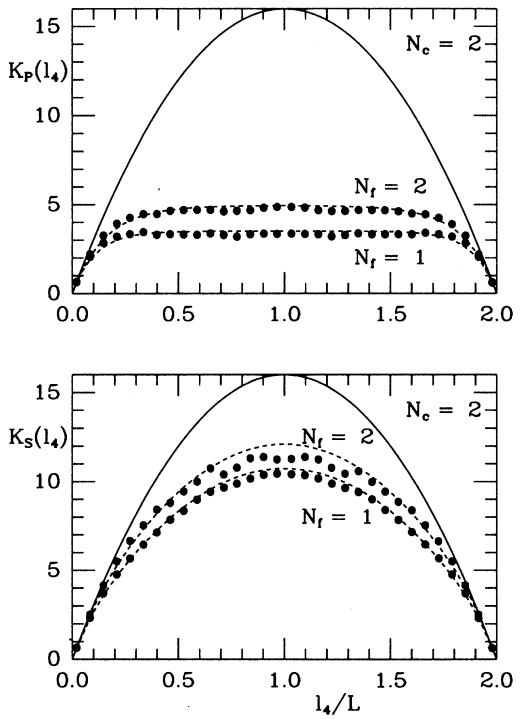

FIG. 2. The pseudoscalar correlator $K_P(l_4)$ (upper figure) and the scalar gluonic correlator $K_S(l_4)$ (lower figure) as a function of the length of the slice, l_4, in the four-direction of total length $2L$. The full line is for randomly positioned instantons and the dashed curves represent results of a fit. All results in this figure are for two colors and one or two massless flavors.

[7] A similar cancellation takes place in many cases, e.g., in [the two-dimensional (2D)] Schwinger model (see [27] for details).

[8] The functional form of this curve, which follows immediately from the binomial distribution of the instantons, is given by $N(l_4/L_4)[1-(l_4/L_4)]$.

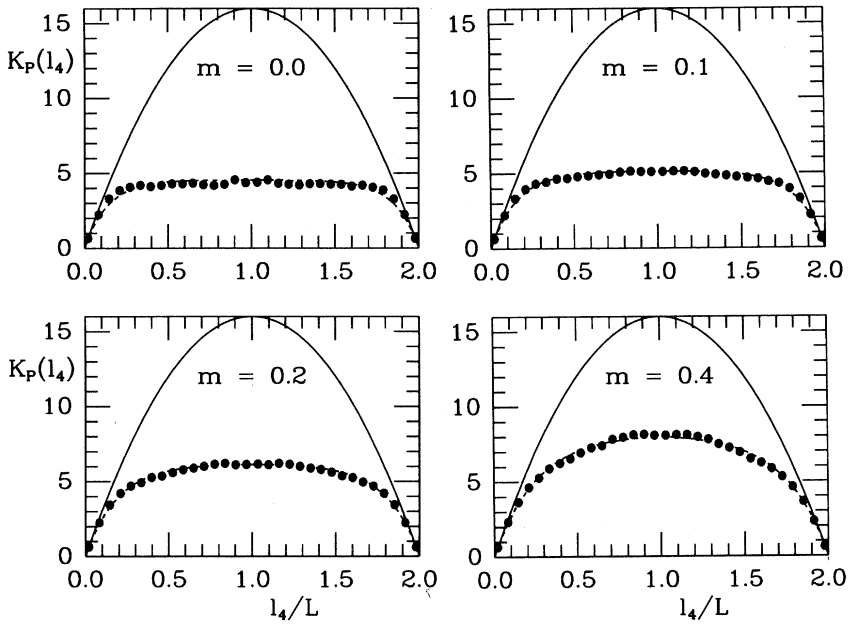

FIG. 3. The mass dependence of the pseudoscalar topological correlator for three colors and two flavors of equal mass (in units of fm^{-1}) given in the label of the figures. For further explanation we refer to the caption of Fig. 2.

In the upper figure of Fig. 2 we compare the cases with *one* and *two* massless quarks, for $N_c = 2$. For massless quarks the correlation function (4.4) reduces to

$$\langle Q(l_4)^2\rangle_{\text{chiral}} = \frac{1-\exp(-m_{\eta'} l_4)}{m_{\eta'}}. \tag{4.8}$$

The dashed curves show a fit of this function to the data points. For $N_f = 1$ and $N_f = 2$ we find $m_{\eta'} = 535$ MeV and $m_{\eta'} = 756$ MeV, respectively. The ratio of the masses is 1.41 which is right on top of the theoretical expectation that $m_{\eta'} \sim \sqrt{N_f}$ [see (B14)]. If we study the susceptibility $\langle Q(l_4)^2\rangle$ as a function of increasing quark mass, which effectively reduces the number of flavors, we therefore expect on the one hand that the η' mass decreases, whereas, on the other hand, it increases because of the explicit contribution of the quark masses.

The quark mass dependence of the topological correlator is studied in Fig. 3. In this case the number of colors is three and we consider two flavors with equal mass (the same instanton configurations as in Fig. 1). For the quark mass we refer to the label of the figure.

In the case of equal quark masses, the fitting formula [that follows from Eq. (B13)] is

$$\langle Q(l_4)^2\rangle = nL^3\left[\alpha^2 l_4\left(1-\frac{l_4}{2L}\right) + (1-\alpha^2)\frac{1-\exp(-m_{\eta'} l_4)}{m_{\eta'}}\right]. \tag{4.9}$$

The value of α obtained from a least-squares fit is 0.0, 0.0, 0.0, 0.19 and $m_{\eta'}$ equals 580, 520, 430, and 340 MeV for quark masses of 0.0, 20.0, 40.0, and 80.0 MeV, in this order. As we already observed in the previous section, our results set a limit on the existence of a critical mass below which we have complete screening. (Again with the disclaimer that the individual parameters are not well determined by the fit.) Only the height of the curves is well determined. Our values for the η' mass are somewhat less than in the previous section, but show the same trend: it *decreases* with the *increasing* quark mass

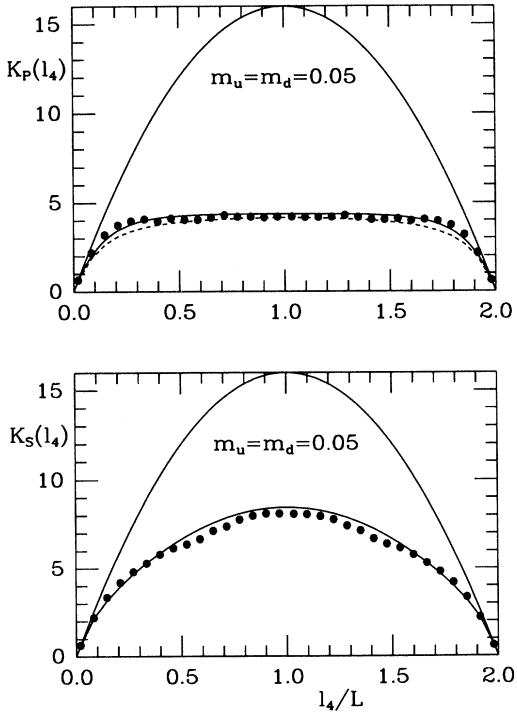

FIG. 4. The pseudoscalar correlator $K_P(l_4)$ (upper figure) and the scalar gluonic correlator $K_S(l_4)$ (lower figure) as a function of the length l_4 of the subvolume for $N_c = 3$, $N_f = 3$, and $m_u = m_d = 10$ MeV and $m_s = 150$ MeV. Further explanation can be found in the caption of Fig. 2.

(for not too large quark masses).

Finally, in Fig. 4, we show results for realistic quark masses,[9] $m_u = m_d = 10$ MeV and $m_s = 150$ MeV.

The dashed line corresponds to effective theory with realistic meson masses and η-η' mixing angle, it agrees with data points quite well. However, our best fit of Eq. (4.4) to the data (shown by the full line) suggest quite different parameters: the pion and the kaon mass to be zero, whereas $m_{\eta'} = 605$ MeV. Clearly, only some combinations of the parameters can really be determined from those data points, not all the individual parameters. In particular, we have found that the fitted curve is very insensitive to the value of the strange quark mass. (And in fact the best fit misses the strange quark contribution to the $m_{\eta'}$.) Note that in naive chiral perturbation theory this meson should possess a strangeness-related mass $m_{\eta'}^{\rm strange} = m_\eta/\sqrt{2} = 388$ MeV. The sum of these two numbers are in the correct region.

V. COMPRESSIBILITY OF THE INSTANTON LIQUID

Let us now proceed to studies of a related gluonic correlation function

$$\Pi_S(x-y) = \left\langle \frac{g^2}{32\pi^2} FF(x) \frac{g^2}{32\pi^2} FF(y) \right\rangle, \tag{5.1}$$

containing the action rather than the topological charge, and therefore counting instantons and anti-instantons equally. The total topological charge in a subvolume V is given by

$$N(V) = \int_V d^4x \frac{g^2}{32\pi^2} FF(x), \tag{5.2}$$

which satisfies that $\langle N(V)\rangle = nV$. For pointlike pseudoparticles we have

$$\frac{g^2}{32\pi^2} FF(x) = \sum_{I=1}^{N} \delta^4(x - X_I). \tag{5.3}$$

For small $|x-y|$ only terms involving the same instanton contribute and we find that

$$\Pi_S(x-y) = n\delta^4(x-y) \quad \text{for } |x-y| \to 0. \tag{5.4}$$

In reality the instantons are not pointlike, and show a repulsive interaction. This leads to the low-energy theorem [38,31,39]

$$\langle [N(V)]^2\rangle - \langle N(V)\rangle^2 = \frac{4}{b}\langle N(V)\rangle, \tag{5.5}$$

where $b = \frac{11}{3}N_c - \frac{2}{3}N_f$ is the standard Gell-Mann–Low coefficient, and the volume is assumed to be large, $V \to \infty$. The compressibility of the instanton liquid is thus equal to $4/b$. As can be seen from (5.4), for relatively small volumes the fluctuation just is proportional to the instanton density n, without the factor $4/b$. How can we understand this in terms of the physical states contributing to the correlation function?

The lowest-lying intermediate state is a "scalar glueball," which we will generically call σ, which presumably has large mass $m_\sigma \sim 1700$ MeV (and should not to be mixed with the quark-based σ of sigma model, at 600 MeV). Using a somewhat different convention than in the pseudoscalar channel the relevant matrix element is

$$\left\langle 0 \left| \frac{g^2}{32\pi^2} FF \right| \sigma \right\rangle = \lambda_\sigma. \tag{5.6}$$

Including also the contribution of the continuum with coupling constant $\lambda_c = \alpha_S^2/32\pi^4$, this results in the correlator

$$\Pi_S(x-y) = \lambda_\sigma^2 D(m_\sigma, |x-y|) + \lambda_c^2 \int_{s_0}^{\infty} ds D(\sqrt{s}, |x-y|) s^2. \tag{5.7}$$

This result contains both perturbative and nonperturbative contributions. However, the correlation function from the instanton liquid calculation only receives contributions from the latter sector. Therefore, we should compare out results to $\Pi_S^{\rm np} \equiv \Pi_S - \Pi_S^{\rm pert}$. The spectral representation of the perturbative contribution is given by

$$\Pi_S^{\rm pert} = \lambda_c^2 \int_0^{\infty} ds D(\sqrt{s}, |x-y|) s^2, \tag{5.8}$$

which results in the nonperturbative correlator

$$\Pi_S^{\rm np} = \lambda_\sigma^2 D(m_\sigma, |x-y|) - \lambda_c^2 \int_0^{s_0} ds D(\sqrt{s}, |x-y|) s^2. \tag{5.9}$$

In the same way as for the topological correlator we define the correlator, $K_S(l_4)$, as the *variance* of the total field strength inside the box $H(l_4)$. Numerically, this correlator can be evaluated again by simply counting the number of instantons inside the box. It is related to $\Pi_S^{\rm np}$ by

$$K_S(l_4) = L^3 \int_{L^3} d^3x \int_{-l_4}^{l_4} dt (l_4 - |t|) \Pi_S^{\rm np}((\vec{x}^2 + t^2)^{1/2}). \tag{5.10}$$

Using the correlators (5.7) and (5.8) we find

[9] Of course, for any finite volume simulation the value of m_f cannot be taken arbitrary small: the minimum possible value of m is the point where the m derivative of the condensate vanishes. For feasible columns we work with $m_f = 0.5 \approx 10$ MeV, being small compared to hadronic masses but still considerably larger than the light quark masses in the real world.

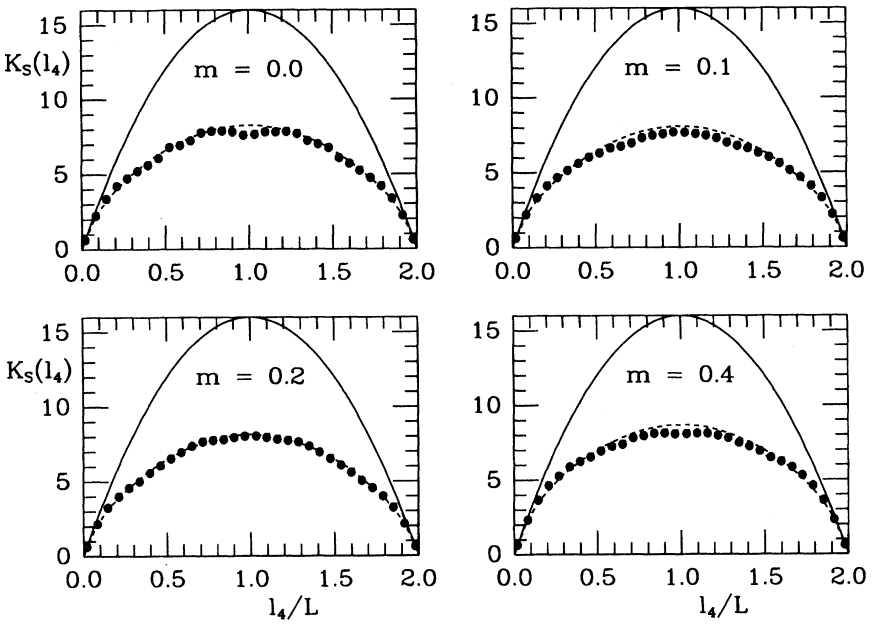

FIG. 5. The mass dependence of the scalar topological correlator, $K_S(l_4)$, for three colors and two flavors of equal mass (in units of fm^{-1}) given in the label of the figures. For further explanation we refer to the caption of Fig. 2.

$$K_S(l_4) = \frac{\lambda_\sigma^2}{m_\sigma^2} L^3 \left(l_4 - \frac{1-\exp(-m_\sigma l_4)}{m_\sigma} \right) - \lambda_c^2 L^3 \int_0^{s_0} \frac{1}{s} \left(l_4 - \frac{1-\exp(-l_4\sqrt{s})}{\sqrt{s}} \right) s^2 ds. \tag{5.11}$$

For large volumes the low-energy theorem (5.5) should be obeyed. This leads to the relation

$$\frac{\lambda_\sigma^2}{m_\sigma^2} - \frac{1}{2}\lambda_c^2 s_0^2 = \frac{4}{b} n. \tag{5.12}$$

In the lower part of Figs. 2, 4, and 5, we show results for the scalar correlators. The full lines in all figures correspond to a random positioning of the instantons. For infinite volume we would get a straight line, but finite size corrections turn it into a parabola. The numerical results are represented by dots. The dashed line is a fit using a combination of (5.11) and (5.12) with the linear large l_4 behavior replaced by its parabolic finite size counterpart. Explicitly, the fitting function is given by

$$f(l_4) = \frac{N}{2L} \left[\frac{4}{b} l_4 \left(1 - \frac{l_4}{2L} \right) - \lambda^2 \frac{1-\exp(-m_\sigma l_4)}{m_\sigma} - \frac{4}{\sqrt{s_0}} \left(\lambda^2 - \frac{4}{b} \right) F(l_4\sqrt{s_0}) \right], \tag{5.13}$$

where the "missing continuum function" F follows from the integral in (5.11):

$$F(x) = -\frac{1}{3} + \frac{2}{x^3} - \left(\frac{1}{x} + \frac{2}{x^2} + \frac{2}{x^3} \right) \exp(-x). \tag{5.14}$$

This fitting function both reproduces the short distance behavior (5.4) and the low-energy theorem (5.5). The constant λ is related to λ_σ by $\lambda^2 = \lambda_\sigma^2/(m_\sigma^2 n)$.

Results for $N_c = 2$ and $N_f = 1$ or $N_f = 2$ are shown in Fig. 2. The fitted values of λ_σ/m_σ equal 1.09 fm $^{-2}$ in both cases, the values of $\sqrt{s_0}$ are 1700 and 1215 MeV and m_σ turns out to be as large as 34 and 31 GeV, respectively. This very large value is no surprise. The correlator (5.1) was evaluated by counting the number of pseudoparticles inside a box which is equivalent to approximating the profile of the instantons by delta functions. The glueball contribution is indeed a strongly peaked one with a fitted value of $\lambda_\sigma^2/m_\sigma^2 = 1.19n$.

In Fig. 5 we study the current quark mass dependence for $N_c = 3$ and two flavors of equal mass. For current quark masses equal to 0, 20, 40, and 80 MeV we find a fit with λ_σ/m_σ equal 1.16, 1.12, 1.13, and 1.39 fm^{-2}, respectively.[10] For the continuum parameter $\sqrt{s_0}$ we find the values 1.8, 2.2, 1.8, and 3.3 GeV, in the same order.

Finally, in the lower figure of Fig. 3, we show K_S for realistic values of the quark masses (see caption). Also in this case we find a best fit with λ_σ/m_σ equal to 1.2 fm^{-2} (and a very large glueball mass of 19 GeV). For the continuum parameter we find the very reasonable value of 2.3 GeV. This large value implies that the continuum only contributes at small volumes, while the bulk of the results discussed in this section are well described by the first term in (5.13).

VI. CONCLUSIONS

We have presented a detailed study of the volume dependence of the fluctuations of the topological charge in

[10]The fitted values of the glueball masses are 21, 18, 27, and 13 GeV. Again these large values are unphysical, and related to the delta function short distance behavior of the correlator.

an interaction instanton liquid model of the QCD vacuum. As was expected, we found that these fluctuations are screened for a sufficiently large box and sufficiently small quark masses due to the fermion-induced interaction between instantons. The phenomenon disappeared gradually as the quark mass increases from zero. An upper limit for the Samuel's critical mass value is set to about 20 MeV. Furthermore, the results for the *correlated* instanton liquid have shown that correlations are essential for reproducing the $m_{\eta'}$ and its dependence on the number of colors and flavors.

As a by-product, we have obtained a formula similar to the Witten-Veneziano formula, but the topological susceptibility that enters into it is not the large volume limit but rather the small volume limit in the presence of dynamical fermions.

We also present results for the fluctuations of total number of instantons in the finite box. The results clearly indicate that the instanton liquid is not an ideal gas, but a liquid with an important repulsive interaction. The results agree very well with the Novikov-Shifman-Vainshtein-Zakharov (NSVZ) low-energy theorem, and provide constraints for the parameters of the physical particles in the scalar channel.

Finally, let us emphasize that the method to evaluate the η' parameters proposed in this work can be applied to lattice QCD calculations with dynamical fermions as well. Straightforward evaluation of the quark propagators can be substituted by measurements of the topological charge in a finite box, which may be much easier to do.

ACKNOWLEDGMENTS

This work was supported in part by the U.S. department of energy under Grant DE-FG02-88-ER40388. We acknowledge the NERSC at Lawrence Livermore where most of the computations presented in this paper were performed. Th. Schäfer and I. Zahed are acknowledged for useful discussions.

APPENDIX A: FERMIONIC OVERLAP MATRIX ELEMENTS FOR THE STREAMLINE ANSATZ

In this appendix we calculate the overlap matrix elements of the Dirac operator between fermionic zero modes of an instanton and an anti-instanton in the streamline field configuration.

For the streamline configuration we use the Yung ansatz [35] which is very close to the exact streamline solution (see [33]) and is given by

$$A_\mu^a \frac{\tau_2}{2} = U_A \tau_a \eta^a_{\mu\nu} x_\nu \frac{1}{x^2+\rho^2\lambda} U_A^{-1} + U_I \sigma_\mu^- \hat{R}_\mu \tau_a \eta^a_{\mu\nu} x_\nu \frac{\rho^2/\lambda}{x^2(x^2+\rho^2/\lambda)} \sigma_\mu^+ \hat{R}_\mu U_I^{-1}, \tag{A1}$$

where $\hat{R}_\mu = R_\mu/R$. After a combined space inversion, scale transformation and translation of the coordinates

$$x_\mu \to s x_\mu/x^2 - c_\mu, \tag{A2}$$

and the fields

$$A_\mu^a \to \frac{s}{x^2}\left(\delta_{\mu\nu} - 2\frac{x_\mu x_\nu}{x^2}\right) A_\mu^a \left(s\frac{x_\mu}{x^2} - c_\mu\right), \tag{A3}$$

and a gauge transformation, the field configuration (A1) can be written as the sum of an instanton and an anti-instanton in the singular gauge and several other terms that vanish for large separation. The positions and the sizes of the pseudoparticles are given by

$$x_{I\nu} = \frac{s c_\nu}{c^2+\rho^2/\lambda}, \quad x_{A\nu} = \frac{s c_\nu}{c^2+\rho^2\lambda}, \tag{A4}$$

$$\rho_I = \frac{s\rho/\sqrt{\lambda}}{c^2+\rho^2/\lambda}, \quad \rho_A = \frac{s\rho\sqrt{\lambda}}{c^2+\rho^2\lambda}. \tag{A5}$$

The separation R_μ between an instanton and an anti-instanton is defined by

$$R_\mu = x_\mu^I - x_\mu^A. \tag{A6}$$

For the derivation of the inverse transformation we refer to [33]. The result for λ in terms of the sizes and the separation is given in (2.4) in the main text of this paper. The orientations of the instanton and the anti-instanton in the streamline configuration at finite R is determined from their values for $R \to \infty$. With this definition U_A and U_I in (A1) are the usual orientation matrices. Note that a space inversion transforms an instanton into an anti-instanton and vice versa.

The overlap matrix elements of the Dirac operator $i\gamma D$, between fermionic zero modes ϕ_I and ϕ_A, are defined by

$$T_{IA} = \int d^4x \phi_I^\dagger(x) i\gamma D \phi_A(x). \tag{A7}$$

Apart from the invariance under gauge transformations, this matrix is also invariant under the conformal transformations (A2) and (A3) supplemented by the transformation

$$\psi(x) \to s^{3/2} \frac{\gamma\cdot x}{x^4} \psi\left(s\frac{x_\mu}{x^2} - c_\mu\right) \tag{A8}$$

for the fermionic fields. This allows us to evaluate it for the conformally symmetric field configuration (A1). Noting that instantons change into anti-instantons under conformal transformations, the zero mode corresponding to the first term in (A1) (an instanton zero mode in the regular gauge) is

$$\phi_A(x) = \frac{1}{\pi}\frac{\rho\sqrt{\lambda}}{(x^2+\rho^2\lambda)^{3/2}} U_A \epsilon_I, \tag{A9}$$

the zero mode corresponding to the second term (an anti-instanton zero mode in the singular gauge) is

$$\phi_I(x) = \frac{1}{\pi}\frac{\rho/\sqrt{\lambda}}{(x^2+\rho^2/\lambda)^{3/2}} \frac{\gamma\cdot x}{|x|} U_I (-i)\sigma^- \cdot \hat{R}\epsilon_I. \tag{A10}$$

In both cases the 4×2 matrix ϵ is given by

$$\epsilon_I = \epsilon_A = \frac{1}{\sqrt{2}} \begin{pmatrix} 0 & 1 \\ -1 & 0 \\ 0 & 1 \\ -1 & 0 \end{pmatrix}. \tag{A11}$$

One more subtlety should be mentioned. Under the conformal transformations (A2) the norm of the zero modes is not invariant,

$$\int d^4x \phi_A^\dagger(x)\phi_A(x) \to \frac{s}{c^2 + \rho^2\lambda}, \tag{A12}$$

instead of 1 for (A9) and (A10). This can be shown most easily by performing the transformation (A2) on the explicit expressions (A9) and (A10). The norm of ϕ_I transforms as

$$\int d^4x \phi_I^\dagger(x)\phi_I(x) \to \frac{s}{c^2 + \rho^2/\lambda}. \tag{A13}$$

The matrix elements of the *normalized* zero modes are therefore not invariant under (A2). However, comparison to (A5) tells us that the matrix elements of the normalized zero modes transform according to

$$\rho T_{IA} \to (\rho_I \rho_A)^{1/2} T_{IA}. \tag{A14}$$

The calculation of the matrix element (A7) can be further simplified by adding and subtracting $i\gamma\partial$ to $i\gamma D$ and using that ϕ_I and ϕ_A are zero mode solutions of the Dirac equation. The result is

$$T_{IA}\rho = -\rho \int d^4x \phi_I^\dagger(x) i\gamma\partial\phi_A(x). \tag{A15}$$

After differention with respect to ∂_μ the Dirac-color trace in (A15) becomes

$$\mathrm{Tr}(\epsilon_A^\dagger \gamma \cdot x \ \gamma \cdot x \ i\sigma_\mu^+ \cdot \hat{R} \ U_I^{-1} U_A \epsilon_I)$$

$$= x^2 \mathrm{Tr}(i\sigma_\mu^+ \cdot R \ U_I^{-1} U_A). \tag{A16}$$

Using the spherical symmetry, the integral can be written as

$$T_{IA\rho} = 6i\mathrm{Tr}(i\sigma_\mu^+ \cdot \hat{R} \ U_I^{-1} U_A) \times \int_0^\infty dx \frac{x^4}{(x^2 + 1/\lambda)^{3/2}(x^2 + \lambda)^{5/2}}, \tag{A17}$$

which, after a change of variables, agrees with the expression (2.4) in the text.

For large separation the conformally invariant parameter $\lambda \to \infty$ in which case the integral reduces to

$$\frac{1}{2}\int_0^\infty \frac{dz}{(z+\lambda)^{5/2}} = \frac{1}{3\lambda^{3/2}}, \tag{A18}$$

resulting in the asymptotics

$$(\rho_I \rho_A)^{1/2} T_{IA} \approx -2(\rho_I \rho_A)^{3/2} \frac{\mathrm{Tr}\sigma_\mu^+ \cdot \hat{R} U_I^{-1} U_A}{R^3} \tag{A19}$$

for $R \to \infty$, in agreement with the asymptotic result for the sum ansatz as obtained by Diakonov and Petrov [31]. (Note that their definition of the overlap matrix element differs by a minus sign from ours.)

APPENDIX B: TOPOLOGICAL CORRELATORS IN EFFECTIVE FIELD THEORY

The topological charge density is defined by

$$Q(x) = \frac{g^2}{32\pi^2} F\tilde{F}(x), \tag{B1}$$

where F is the field strength tensor. The topological charge $Q(V)$ in four-volume V is obtained by integration of $Q(x)$ over V. The fluctuations of the topological charge in a given box are determined by the topological correlation function defined by

$$\Pi_P(x-y) = \left\langle \frac{g^2}{32\pi^2} F\tilde{F}(x) \frac{g^2}{32\pi^2} F\tilde{F}(y) \right\rangle. \tag{B2}$$

In this Appendix we will derive this correlator from the effective low-energy chiral Lagrangian [40] and its interaction with the topological charge Q. This derivation is based on work in Refs. [18–20]. The main additional ingredient is that we include the η-η' mixing in our derivation.

The topological charge density couples to the pseudoscalar singlet meson channel, and, for a diagonal mass matrix with $m_u = m_d$, only the η-η' mixing part of the effective pseudoscalar Lagrangian is of relevance.[11] This part, which involves only the diagonal (SU(3)-flavor fields ϕ_0 and ϕ_8, is given by [23,40,41,32,42]

$$\mathcal{L}_{\mathrm{eff}} = -i \int d^4x \frac{\sqrt{2N_f}}{f} \phi_0 Q + \mathcal{L}(\phi_0, \phi_8), \tag{B3}$$

with

$$\mathcal{L}(\phi_0, \phi_8) = \frac{1}{2} \begin{pmatrix} \phi_0 \\ \phi_8 \end{pmatrix} (\nabla^2 + \mathcal{M}^2) \begin{pmatrix} \phi_0 \\ \phi_8 \end{pmatrix}, \tag{B4}$$

and the square of the mass matrix [23]

$$\mathcal{M}^2 = \begin{pmatrix} \frac{2}{3}m_K^2 + \frac{1}{3}m_\pi^2 & \frac{2\sqrt{2}}{3}(m_\pi^2 - m_K^2) \\ \frac{2\sqrt{2}}{3}(m_\pi^2 - m_K^2) & \frac{4}{3}m_K^2 - \frac{1}{3}m_\pi^2 \end{pmatrix}. \tag{B5}$$

The normalization of the fields and the coupling constant f will be discussed below.

In the dilute gas approximation the instanton partition function is given by [43,18]

---

[11] In fact, there is another state with the quantum numbers of the η', η (1430) and formerly called ι, which gives a comparable contribution to this correlation function (see discussion in [6]). We do not include it here, because it is hardly possible to extract any information about this state from the data sample discussed in this paper.

$$Z = \sum_{N_+N_-} \frac{\kappa^{N_++N_-}}{N_+!N_-!} \prod_{i=1}^{N} d^4z_i \exp\left(-\int d^4x \mathcal{L}_{\text{eff}}\right). \quad \text{(B6)}$$

The constant κ was calculated to one-loop order in [2]. Treating the instantons as pointlike objects, the topological charge density is given by $Q(x) = \sum Q_i \delta(x - z_i)$. This allows us to perform the sum over N_+ and N_- in the partition function. Our final effective Lagrangian is obtained by expanding the resulting cosine function to second order (weak field approximation):

$$\mathcal{L}_{\text{eff}} = -2\kappa + \kappa \frac{2N_f}{f^2}\phi_0^2 + \mathcal{L}(\phi_0, \phi_8). \quad \text{(B7)}$$

The constant κ can be traded for the average pseudoparticle density by differentiating both (B6) and (B7) with respect to κ. We find

$$2\kappa = \left\langle \frac{N}{V} \right\rangle \equiv n. \quad \text{(B8)}$$

The topological correlator (B2) can be obtained by integrating out the meson fields. However, it is somewhat simpler to write the correlator in terms of functional derivatives with respect to ϕ_0 of the first term in the Lagrangian (B3) and performing the differentiation after the sum over the instantons, i.e., on the second term in (B7). The correlator can be expressed as

$$\langle Q(x)Q(y)\rangle = n\delta^4(x-y) - n^2 \frac{2N_f}{f^2}\langle \phi_0(x)\phi_0(y)\rangle. \quad \text{(B9)}$$

The latter expectation value is most conveniently obtained by diagonalizing the mass matrix $\mathcal{M}$ (including the topological contribution) with eigenvalues identified as $m_{\eta'}$ and m_η and eigenvectors expressed in the η'-η mixing angle according to

$$|\eta'\rangle = \cos\phi|\phi_0\rangle + \sin\phi|\phi_8\rangle, \quad \text{(B10)}$$

$$|\eta'\rangle = \cos\phi|\phi_8\rangle - \sin\phi|\phi_0\rangle. \quad \text{(B11)}$$

For the singlet correlation function we obtain

$$\langle \phi_0(x)\phi_0(y)\rangle = \cos^2(\phi)D(m_{\eta'}, |x-y|) + \sin^2(\phi)D(m_\eta, |x-y|) \quad \text{(B12)}$$

resulting in the topological correlator

$$\langle Q(x)Q(y)\rangle = \frac{f^2}{2N_f} m_{\text{top}}^2 \{\delta^4(x-y) - m_{\text{top}}^2 \times [\cos^2(\phi)D(m_{\eta'}, |x-y|) + \sin^2(\phi)D(m_\eta, |x-y|)]\}, \quad \text{(B13)}$$

where the scalar propagator is given by $D(m,x) = mK_1(mx)/(4\pi^2 x)$. For convenience we have introduced the topological mass

$$m_{\text{top}}^2 \equiv \frac{2N_f n}{f^2} = m_{\eta'}^2 + m_\eta^2 - 2m_K^2, \quad \text{(B14)}$$

where the latter identity follows from the invariance of the trace of the mass matrix under diagonalization. The η' contribution to this correlation function can also be derived from the pseudoscalar singlet spectral function using the matrix element $\langle 0|Q(x)|\eta'\rangle = m_{\eta'}^2 f_{\eta'}/\sqrt{2N_f}$. This defines the constant and the normalization of the fields in our effective Lagrangian.

It is interesting to calculate the topological susceptibility

$$\chi \equiv \lim_{V\to\infty} \frac{\langle [\int d^4x Q(x)]^2\rangle}{V} = n\left(1 - \frac{(\frac{4}{3}m_K^2 - \frac{1}{3}m_\pi^2)m_{\text{top}}^2}{(\frac{4}{3}m_K^2 - \frac{1}{3}m_\pi^2)m_{\text{top}}^2 + 2m_K^2 m_\pi^2 - m_\pi^4}\right). \quad \text{(B15)}$$

We observe the well-known fact that the topological charge is completely screened if *one* massless quark is present. Note that this formula has been derived for $m_u = m_d$. Indeed, for zero light quark masses we have $m_\pi = 0$ and $\chi = 0$. If $m_s = 0$ we have that $m_\pi^2 = 2m_K^2$ and also $\chi = 0$.

As has been particularly emphasized by Dowrick and McDoughal [19], we can look at the effective Lagrangian in a different way. Namely we integrate over the pseudoscalar singlet and are left with a residual instanton interaction. In the present case, with the SU(3)-mixing angle taken into account, we have to integrate over both ϕ_0 and ϕ_8. This results in the effective Lagrangian

$$\mathcal{L} = \frac{1}{2}\frac{2N_f}{f^2}\sum_{i\neq j} Q_iQ_j\left(\frac{2}{3}D(m_\pi, |z_i - z_j|) + \frac{1}{3}D(\sqrt{2m_K^2 - m_\pi^2}, |z_i - z_j|)\right), \quad \text{(B16)}$$

where we have subtracted the infinite self-energy terms (for $z_i = z_j$). The range of the interaction between the pseudoparticles is of order of $1/m_\pi$. Although it is believed that a Yukawa interaction is not strong enough [44] to induce a plasma phase, the relatively long range interaction justifies the study of the scenario recently proposed by Samuel [16].

[1] A. A. Belavin, A. M. Polyakov, A. A. Schwartz, and Yu. S. Tyupkin, Phys. Lett. **59B**, 85 (1975).

[2] G. 't Hooft, Phys. Rev. Lett. **37**, 8 (1976); Phys. Rev. D **14**, 3432 (1976).

[3] E. V. Shuryak and J. J. M. Verbaarschot, Nucl. Phys. **B410**, 37 (1993).

[4] E. V. Shuryak and J. J. M. Verbaarschot, Nucl. Phys. **B410**, 55 (1993).

[5] T. Schäfer, E. V. Shuryak, and J. J. M. Verbaarschot, Nucl. Phys. **B412**, 143 (1994).

[6] E. V. Shuryak, Rev. Mod. Phys. **65**, 1 (1993).

[7] M. C. Chu, J. M. Grandy, S. Huang, and J. W. Negele, Phys. Rev. Lett. **70**, 255 (1993).

[8] T. Schäfer and E. V. Shuryak, Phys. Rev. D **50**, 478

(1994).
[9] B. Berg, Phys. Lett. **114B**, 475 (1981); M. Teper, in *Lattice '90*, Proceedings of the International Symposium, Tallahassee, Florida, edited by U. M. Heller, A. D. Kennedy, and S. Sanielevici [Nucl. Phys. B (Proc. Suppl.) **20**, 159 (1991)].
[10] M. C. Chu, J. M. Grandy, S. Huang, and J. W. Negele, Phys. Rev. D **49**, 6039 (1994).
[11] E. V. Shuryak, Nucl. Phys. **B203**, 116 (1982); **B203**, 140 (1982); **B203**, 237 (1982).
[12] T. Schäfer, E. V. Shuryak, and J. J. M. Verbaarschot, Nucl. Phys. **B412**, 143 (1994).
[13] T. Schäfer, E. V. Shuryak, and J. J. M. Verbaarschot, Mesons in the correlated instanton vacuum (unpublished).
[14] R. Peccei and H. Quinn, Phys. Rev. Lett. **38**, 1440 (1977).
[15] G. Schierholz, "Towards a dynamical solution of the strong CP problem," DESY Report No. DESY 94-031, 1994 (unpublished).
[16] S. Samuel, Mod. Phys. Lett. A **7**, 2007 (1992).
[17] S. Weinberg, Phys. Rev. D **11**, 3583 (1975).
[18] G. 't Hooft, Phys. Rep. **142**, 357 (1986).
[19] N. J. Dowrick and N. A. Mcdougall, Phys. Lett. B **285**, 269 (1992); Nucl. Phys. **B399**, 426 (1993).
[20] H. Kikuchi and J. Wudka, Phys. Lett. B **284**, 111 (1992).
[21] I. Zahed, Nucl. Phys. **B427**, 561 (1994).
[22] E. Witten, Nucl. Phys. **156**, 269 (1979).
[23] G. Veneziano, Nucl. Phys. **B159**, 213 (1979).
[24] J. Smit and J. Vink, Nucl. Phys. **B284**, 234 (1987).
[25] Y. Kuramashi, M. Fukugita, H. Mino, M. Okawa, and A. Ukawa, Phys. Rev. Lett. **72**, 3448 (1994).
[26] T. Schäfer and E. V. Shuryak, "Glueballs and Instantons," SUNY-NTG report (unpublished).
[27] A. Smilga, Phys. Rev. D **46**, 5598 (1992).
[28] E. V. Shuryak, Nucl. Phys. **B302**, 559 (1988); **B302**, 574 (1988); **B302**, 599 (1988).
[29] E. Shuryak, Nucl. Phys. **B319**, 511 (1989); **B319**, 521 (1989), **B328**, 85 (1989); **B328**, 102 (1989).
[30] E. V. Shuryak and J. J. M. Verbaarschot, Nucl. Phys. **B364**, 255 (1991).
[31] D. I. Diakonov and V. Yu. Petrov, Nucl. Phys. **B245**, 259 (1984); **B272**, 457 (1986).
[32] M. A. Nowak, J. J. M. Verbaarschot, and I. Zahed, Nucl. Phys. **B324**, 1 (1989).
[33] J. J. M. Verbaarschot, Nucl. Phys. **B362**, 33 (1991).
[34] E. V. Shuryak and J. J. M. Verbaarschot, Phys. Rev. Lett. **68**, 2576 (1992).
[35] A. V. Yung, Nucl. Phys. **B297**, 47 (1988).
[36] D. I. Diakonov and V. Yu. Petrov, Phys. Rev. D **50**, 266 (1994).
[37] K. Langfeld and H. Reinhardt, Phys. Lett. B **333**, 396 (1994).
[38] V. Novikov, M. Shifman, A. Vainshtein, and V. Zakharov, Nucl. Phys. **B165**, 67 (1980).
[39] E. M. Ilgenfritz, Habilitation Leipzig, 1988.
[40] P. Di Vecchia and G. Veneziano, Nucl. Phys. **B171**, 253 (1980).
[41] D. I. Diakonov and V. Yu. Petrov, Leningrad Report No. LNPI-1153, 1986 (unpublished).
[42] M. A. Nowak, J. J. M. Verbaarschot, and I. Zahed, Phys. Lett. **B228**, 251 (1989); R. Alkofer, M. A. Nowak, J. J. M. Verbaarschot, and I. Zahed, *ibid.* **233**, 205 (1989).
[43] C. G. Callan, R. Dashen, and D. J. Gross, Phys. Rev. D **17**, 2717 (1978).
[44] R. Shrock, in *Quantum Fields on the Computer*, edited by M. Creutz (World Scientific, Singapore, 1992).